Chapter 14

Flammability Studies of Polymer Layered Silicate Nanocomposites: Polyolefin, Epoxy, and Vinyl Ester Resins

J.W. Gilman[1], T. Kashiwagi[1], M. Nyden[1], J.E.T. Brown[1], C.L. Jackson[2], S. Lomakin[1†], E.P. Giannelis[3] and E. Manias[3]

[1]*Fire Science Division and* [2]*Polymers Division, National Institute of Standards and Technology* Gaithersburg, MD 20899 USA*

[3]*Cornell University, Ithaca, NY14853 USA*

ABSTRACT: In the pursuit of improved approaches to fire retarding polymers a wide variety of concerns must be addressed, in addition to the flammability issues. For commodity polymers the low cost of these materials requires that the fire retardant (FR) approach also be of low cost. This limits solutions to the problem primarily to additive type approaches. These additives must be low cost and easily processed with the polymer. In addition, any additive must not excessively degrade the other performance properties of the polymer, and it must not create environmental problems in terms of recycling or disposal of the final product. Polymer layered silicate (PLS) nanocomposites are materials that may fulfil the above requirements for a high performance flame retardant.

PLS nanocomposites are hybrid organic polymer–inorganic materials with unique properties when compared with conventional filled polymers [1]. For example, the mechanical properties of a nylon-6 layered-silicate nanocomposite, with a silicate mass fraction of only 5%, show excellent improvement over those for the pure nylon 6. The nanocomposite exhibits a 40% higher tensile strength, 68% greater tensile modulus, 60% higher flexural strength, and a 126% increased flexural modulus. The heat distortion temperature (HDT) is increased from 65°C to 152°C [2]. In some cases, increased thermal stability, an important property for improving flammability performance, as well as decreased gas permeability, and increased solvent resistance accompany the improved physical properties.

We have reported on the flammability properties of delaminated nylon 6 layered silicate nanocomposites and intercalated polymer layered-silicate nanocomposites prepared from polystyrene (PS) and polypropylene-graft-maleic anhydride (PP-g-MA) [3, 4]. Here, we will briefly review these results and report on our initial studies of the flammability of thermoset PLS nanocomposites: intercalated vinyl ester silicate and intercalated epoxy silicate nanocomposites.

---

* This work was carried out by the National Institute of Standards and Technology (NIST), an agency of the US Government, and by statute is not subject to copyright in the United States.

† NIST Guest Researcher from the Russian Academy of Sciences.

Chemistry and Technology of Polymer Additives. Chapter 14. 1999, Blackwell Science Inc., Malden, MA, Ak-Malaika, S.; Golovoy, A.; Wilkie, C. A., Editors, 249-265 pp, 1999.

14.1 Introduction

Methods of preparing PLS nanocomposites have been developed by several groups over the last decade [1, 2, 5–10]. In general these methods achieve molecular level incorporation of layered silicate (e.g. montmorillonite) into the polymer by addition of a modified silicate; during the polymerization (*in situ*), or to a solvent swollen polymer, or to the polymer melt [1]. Two terms (*intercalated* and *delaminated*) are used to describe the two general classes of nano-morphology that can be prepared. Intercalated structures, where the extended polymer chains are inserted into the gallery space between the individual silicate layers (see Fig. 14.1), are well ordered multi-layered structures. The delaminated (or *exfoliated*) structures result when the individual silicate layers are well dispersed in the organic polymer. The interlayer spacing (20–200 nm) is on the order of the radius of gyration of the polymer. The silicate layers in a delaminated structure may not be as well ordered as in an intercalated structure.

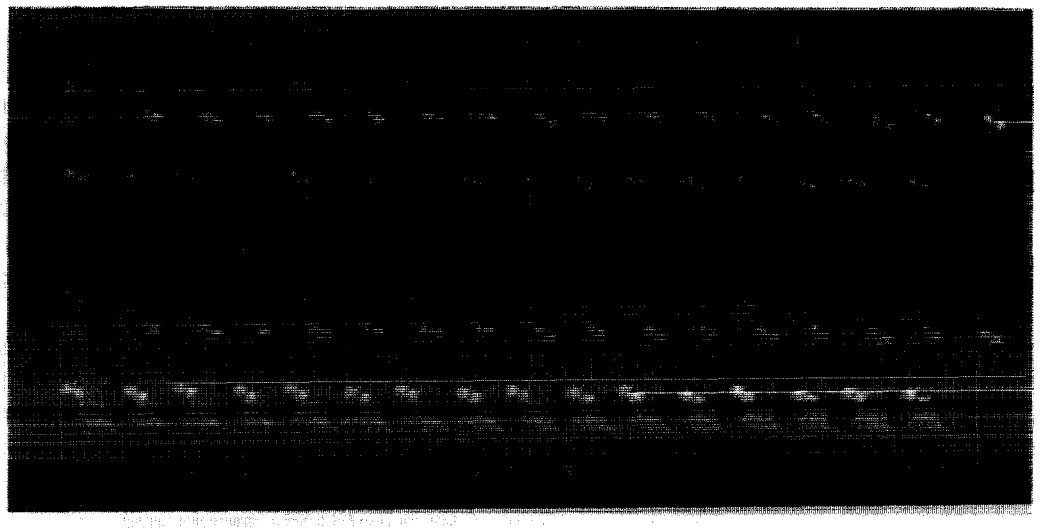

Fig. 14.1 Molecular representation of sodium montmorillonite showing two aluminosilicate layers with the Na^+ cations in the interlayer gap or gallery (1.14-nm layer-to-layer spacing).

Nylon 6 and polycaprolactone silicate-nanocomposites have been prepared through *in situ* ring opening polymerization of monomers. This process requires some re-development of the polymer manufacturing process, and although nylon 6 silicate nanocomposite is commercially available, this approach may not be as attractive for other polymers. Melt intercalation of the polymer directly into the layered silicate has been recently developed. In this process the appropriately modified layered silicate (cation exchanged montmorillonite) and the polymer are combined in the melt to form the nanocomposite [1]. This process is of course most advantageous for thermoplastic polymers. For thermosetting resins the *in situ* polymerization method is still suitable, and the appearance of several publications [5, 10, 11] and patents [12–14] demonstrates that new thermoset silicate-nanocomposites with unique properties can

be prepared. In the case of an unsaturated polyester thermoset resin, the intercalated nanocomposite was shown to have a higher Young's modulus than both the pure polymer and the delaminated nanocomposite [10].

14.2 Previous studies

Thermal analysis (TGA) of several different PLS nanocomposite resin systems has revealed the intriguing result that intercalated nanocomposites are more thermally stable than the delaminated nanocomposites [4, 9, 10]. Molecular dynamics simulations (Fig. 14.2) of the thermal degradation of a series of polypropylene (PP)/graphite nanocomposites recently found that the most pronounced stabilization of the polymer occurred where the graphite layers were separated by 3 nm; that is, had an intercalated structure [15].

Previously, we reported on the flammability properties of several thermoplastic polymer nanocomposites; delaminated nylon 6 layered silicate nanocomposites and intercalated polymer layered-silicate nanocomposites prepared from PS and PP-g-MA [3, 4, 9]. The flammability data for nylon 6, PS and PP-g-MA, and new data on

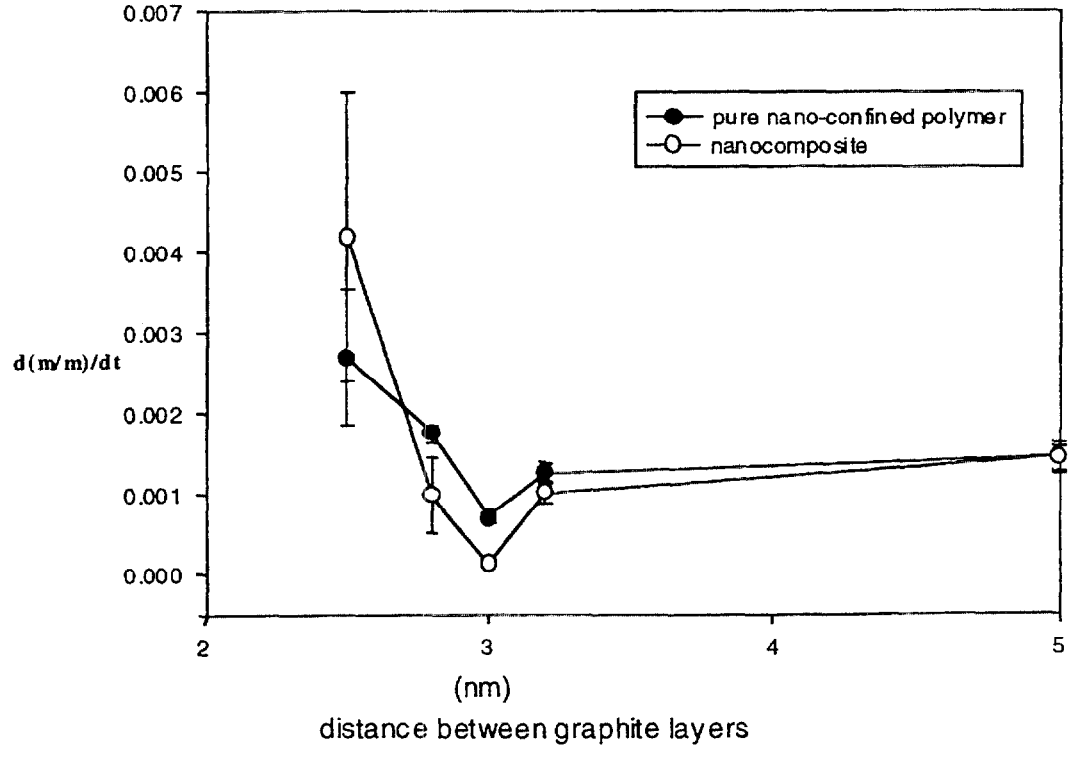

Fig. 14.2 Time averaged mass loss rate *vs.* layer separation distance from molecular dynamics simulations of the thermal degradation for PP/graphite nanocomposite. The solid circles are for the case where there are no non-bonding interactions between the graphite and the PP, and the open circles are for the case where there are non-bonding interactions between the graphite and the PP. Both cases show that the minimum mass loss rate for the polymer occurred where the graphite layers were separated by 3 nm; that is an intercalated structure.

nylon 12 is shown in Table 14.1. The data show that both the peak and average heat release rates (HRR) were reduced significantly for intercalated and delaminated PLS nanocomposites with low mass fraction (2–5%) of silicate. The HRR plots for nylon 6 and nylon 6 silicate nanocomposite (mass fraction 5%) at 35 kW/m^2 heat flux are shown in Fig. 14.3, and are typical of those found for all the PLS nanocomposites in Table 14.1. The nylon 6 nanocomposite has a 63% lower HRR than the pure nylon 6. Furthermore, for the PS silicate nanocomposite the magnitude of improvement in flammability performance is comparable to that found for PS flame retarded using a total mass fraction of 30% of decabromodiphenyl oxide, DBDPO, and antimony trioxide, Sb_2O_3 (see Table 14.1). This is accomplished without as much of an increase

Table 14.1 Cone calorimeter data.

Sample *(structure)*	Residue yield (%) ± 0.5	Peak HRR (Δ%) (kW/m^2)	Mean HRR (Δ%) (kW/m^2)	Mean H_c (MJ/kg)	Mean SEA (m^2/kg)	Mean CO yield (kg/kg)
Nylon 6	1	1010	603	27	197	0.01
Nylon 6 silicate nanocomposite 2% *(delaminated)*	3	686 (32%)	390 (35%)	27	271	0.01
Nylon 6 silicate nanocomposite 5% *(delaminated)*	6	378 (63%)	304 (50%)	27	296	0.02
Nylon 12	0	1710	846	40	387	0.02
Nylon 12 silicate nanocomposite 2% *(delaminated)*	2	1060 (38%)	719 (15%)	40	435	0.02
PS	0	1120	703	29	1460	0.09
PS silicate-mix 3% *(immiscible)*	3	1080	715	29	1840	0.09
PS silicate nanocomposite 3% *(intercalated)*	4	567 (48%)	444 (38%)	27	1730	0.08
PS w/DBDPO/Sb_2O_3 30%	3	491 (56%)	318 (54%)	11	2580	0.14
PP-g-MA	0	2030	861	38	756	0.04
PP-g-MA silicate nanocomposite 5% *(intercalated)*	8	922 (54%)	651 (24%)	37	994	0.05

Heat flux 35 kW/m^2; H_c Heat of combustion; SEA Specific extinction area.

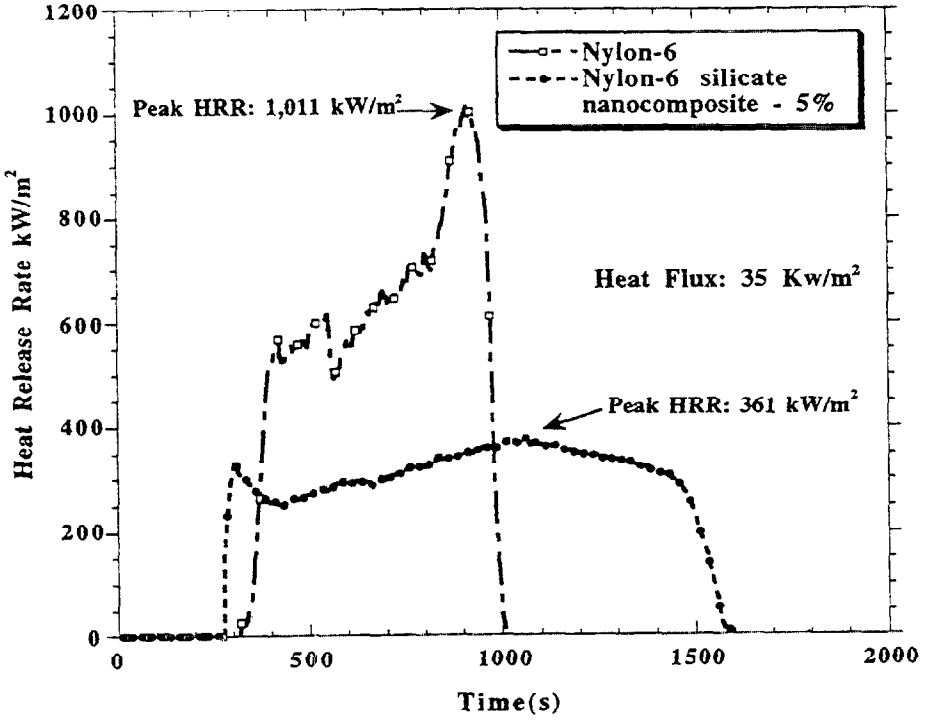

Fig. 14.3 Comparison of the heat release rate (HRR) plot for nylon 6, nylon 6 silicate-nanocomposite (mass fraction 5%) at 35 kW/m^2 heat flux, showing a 63% reduction in HRR for the nanocomposite.

in the soot (SEA) or CO yields. The data also indicate that the rate of mass loss during combustion of the PLS nanocomposite is significantly reduced from the values observed for the pure polymers (see Fig. 14.4). Since the heat of combustion, SEA and carbon monoxide yields are unchanged this suggests that the source of the improved flammability properties of these materials is due to differences in condensed phase decomposition processes and not to a gas phase effect.

14.3 Experimental details

Evaluations of flammability were achieved using the cone calorimeter [16]. The tests were performed at an incident heat flux of 35 kW/m^2 using the cone heater. A heat flux of 35 kW/m^2 represents a typical small-fire scenario [17]. Peak heat release rate, mass loss rate and specific extinction area (SEA) data, measured at 35 kW/m^2, are reproducible to within $\pm 10\%$. The carbon monoxide and heat of combustion data are reproducible to within $\pm 15\%$. The uncertainties for the cone calorimeter are based on the uncertainties observed while evaluating the thousands of samples combusted to date. The cone data reported here are the average of two or three replicated experiments. Cone samples for thermoplastic polymers were prepared by compression moulding the samples (25–55 g) into 75 mm diameter discs, 10–15 mm thick, using a press with a heated mould.

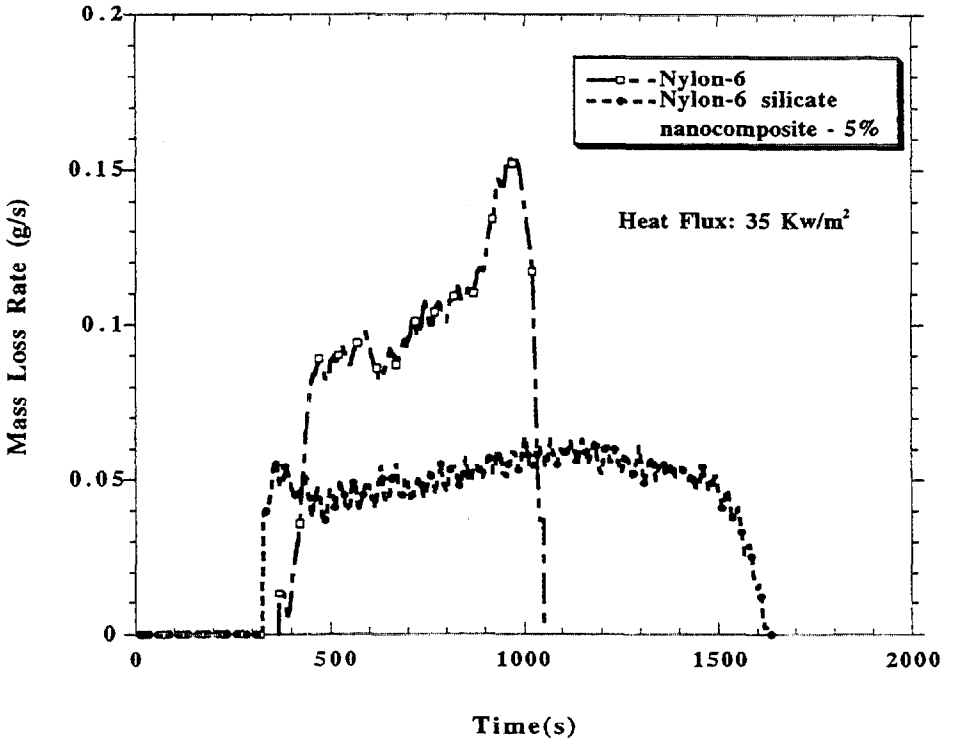

Fig. 14.4 The mass loss rate data for nylon 6, nylon 6 silicate nanocomposites (5%). The curves closely resemble the HRR curves (Fig. 14.3), indicating that the reduction in HRR for the nanocomposites is primarily due to the reduced mass loss rate and the resulting lower fuel feed rate to the gas phase.

The vinyl ester* samples were prepared at room temperature (25°C) by mixing the resin (modified bisphenol-A epoxy based vinyl ester, a combination of a nitrile rubber and bisphenol-A epoxy based vinyl ester, mass fraction of 58% in styrene – Derakane 8084, and bis-A/novolac epoxy based vinyl ester, a combination of bisphenol-A epoxy based vinyl ester and novolac epoxy based vinyl ester, mass fraction of 67% in styrene – Derakane 441, both from Dow Chemical Co., see Fig. 14.5) with the initiator (2-butanone peroxide, mass fraction of 1.25%) the cobalt catalyst (mass fraction of 0.3%, cobalt naphthenate, mass fraction of 6% in mineral spirits, OMG Americas Inc.) and an organically modified silicate (OMS), dimethyl ditallow ammonium montmorillonite, Closite-15A, Southern Clay Products, Inc.) using an overhead mechanical stirrer for 5 minutes. The mixtures were poured into aluminium sample dishes (75 mm diameter × 15 mm depth) and cured at room temperature for 12 h and then post-cured at 70°C for 8 h.

The epoxy samples of diglycidyl ether bisphenol-A based epoxy (DGEBA, DER 331, Dow Chemical Co.) were prepared using a previously published procedure [11]. The mixtures were poured into aluminium sample dishes (75 mm diameter × 15 mm

* Certain commercial equipment, instruments, materials, services or companies are identified in this chapter in order to specify adequately the experimental procedure. This in no way implies endorsement or recommendation by NIST.

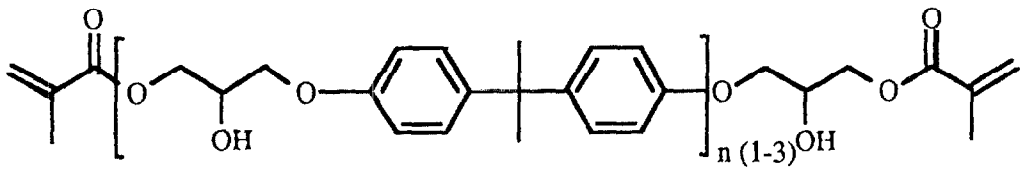

bisphenol-A epoxy vinyl ester resin

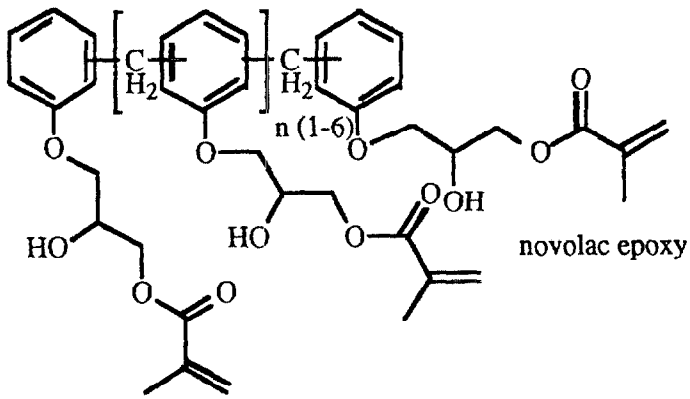

novolac epoxy vinyl ester resin

Fig. 14.5 Vinyl ester resin chemical structures.

depth) and cured at room temperature for 18 h and then post-cured at 100°C for 3 h. Methylenedianiline (MDA) and benzyldimethylamine (BDMA) were used as curing agents. The OMS used was dimethyl ditallow ammonium montmorillonite.

Nylon 6 and nylon 6 silicate nanocomposites (silicate mass fraction of 2% and 5%), nylon 12 and nylon 12 silicate nanocomposites (silicate mass fraction of 2%) were obtained from UBE industries and were used as received.

Preparation of PS-silicate-nanocomposite (silicate mass fraction of 3%) was accomplished by melt blending PS (Styron 6127, Dow Chemical Co.) with dimethyl dioctadecyl ammonium-exchanged montmorillonite [1]. This yields a nanocomposite with the intercalated structure. The intergallery spacing, by X-ray diffraction, XRD, is 3.1 nm ($2\theta = 2.6°$). The immiscible PS-silicate mix, where the silicate is only mixed in at the primary-particle size scale ($\sim 5\,\mu m$), is prepared under the same melt blending conditions except the alkyl ammonium used to compatibilize the montmorillonite has only one octadecyl R group instead of two. This renders the ion exchanged montmorillonite slightly less organophilic and intercalation does not occur.

Preparation of PP-g-MA-silicate-nanocomposite (silicate mass fraction of 5%) by melt blending, was accomplished by pressing the PP-g-MA mixed with the dimethyl ditallow ammonium-exchanged montmorillonite at 160°C for 30 minutes using a Carver press, followed by heating in a vacuum oven for several hours at 160°C. This yields a nanocomposite with the intercalated structure. The intergallery spacing, by XRD analysis, is 3.6 nm. PP-g-MA (m.p. 152°C) was purchased from Aldrich and contains a mass fraction of 0.6% maleic anhydride. It has a melt index of 115 g/600 s and a Mw of ~10K, Mn ~5K.

X-ray diffraction (XRD) spectra were collected on a Phillips diffractometer using Cu Kα radiation (λ = 0.1505945 nm). Powder samples were ground to a particle size of less than 40 μm. Solid polymer-silicate monoliths were typically 14 mm by 14 mm with a 2 mm thickness.

For the transmission electron microscopy (TEM), the char was broken into small pieces, embedded in an epoxy resin (Epofix), and cured overnight at room temperature. Ultra-thin sections were prepared with a 45° diamond knife at room temperature using a DuPont-Sorvall 6000 ultramicrotome. Thin sections (nominally 50–70 nm) were floated onto water and mounted on 200-mesh carbon-coated copper grids. Bright-field TEM images were obtained with a Philips 400T microscope operating at 120 kV, utilizing low-dose techniques.

14.4 Results and discussion

Epoxy and vinyl ester resin systems represent a large fraction of the commercial thermoset polymer, coating, and composite markets [18, 19]. A reduction in the flammability of these inherently highly flammable materials should increase their use. For the purpose of determining the flammability properties of thermoset PLS nanocomposites, especially the intercalated type, two intercalated vinyl ester nanocomposites and two intercalated epoxy nanocomposites were prepared and studied.

14.5 Characterization of nanocomposites by XRD

The microstructure of the epoxy and vinyl ester nanocomposites was characterized using XRD. The XRD patterns, which reveal the intercalated structure of the modified-bisphenol-A (MBA) vinyl ester silicate nanocomposite and the bis-A/novolac (BAN) vinyl ester silicate nanocomposite, are shown in Fig. 14.6. The interlayer spacing for the MBA nanocomposite is 4.8 nm which represents a 1.5 nm expansion of the interlayer spacing of the silicate layers present in the original organically modified montmorillonite. The interlayer spacing for the BAN nanocomposite is 6.2 nm, which represents a 2.9 nm expansion of the interlayer spacing of the silicate layers. The different degree of intercalation for these two vinyl ester systems is most likely due to the different structures of the components of the formulations, shown in Fig. 14.5, and the resulting polarity and conformational mobility differences.

The XRD characterization of the DGEBA epoxy silicate nanocomposites, cured with either MDA or BDMA, shown in Fig. 14.7, confirms intercalated structures, with interlayer spacings of 3.5 nm and 4.3 nm, respectively. These results parallel previously published work where MDA/DGEBA epoxy silicate nanocomposite exhibited less expansion of the silicate spacing than the BDMA/DGEBA epoxy silicate nanocomposite [11]. It was proposed that the MDA, a diamine, could bridge the silicate layers and thereby prevent complete delamination. The BDMA, a

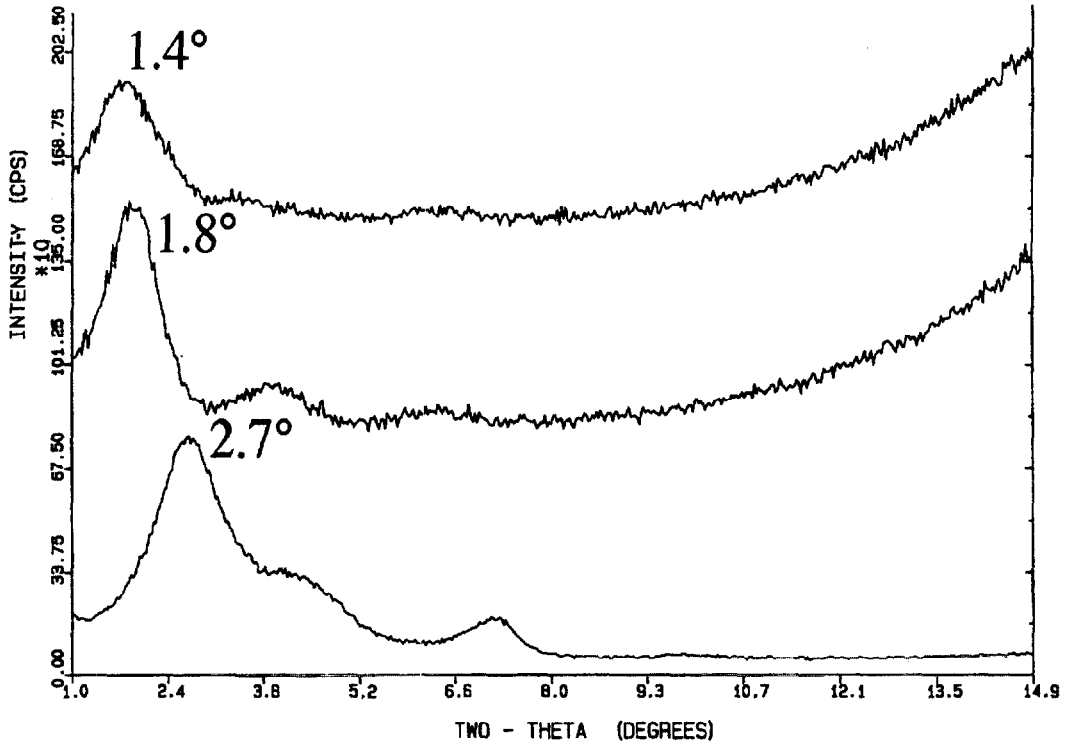

Fig. 14.6 XRD patterns of: pure OMS, dimethyl ditallow ammonium-montmorillonite (*bottom*: $2\theta = 2.7°$, layer spacing 3.3 nm); cured modified-bisphenol-A epoxy based vinyl ester silicate nanocomposite (*middle*: 6% silicate, $2\theta = 1.8°$, layer spacing 4.8 nm) and cured bis-A/novolac epoxy based vinyl ester silicate nanocomposite (*top*: 6% silicate, $2\theta = 1.4°$, layer spacing 6.2 nm).

monoamine, would not have this limitation. In the previous system however, the BDMA/DGEBA nanocomposite was fully delaminated whereas it is only intercalated here. The reason for this difference lies in the different alkyl ammonium montmorillonites used. In the previous study where the BDMA/DGEBA nanocomposite delaminated, the OMS used was bis(hydroxyethyl) methyl tallow montmorillonite. The hydroxyethyl groups in this OMS react with the oxirane rings of the DGEBA aiding in the dispersion of the silicate in the resin. The resulting epoxy network contains chemical bonds to the alkyl ammonium cation and therefore an ionic tether to the silicate [11]. The strength of this ionic tether between the polymer and the silicate was found to have a direct relationship to the tensile strength of the nylon 6 nanocomposites [2]. We used an OMS without reactive functionality (dimethyl ditallow ammonium montmorillonite). This results in a cured DGEBA nanocomposite without an ionic tether to the silicate for both the MDA and BDMA cured epoxies. It should be noted that since the MDA contains four active N—H hydrogens it can react directly as a crosslinking agent with DGEBA. The BDMA contains no active N—H, and it acts only as a catalyst for the homopolymerization of DGEBA. This results in formation of a purely polyether network for the BDMA/DGEBA epoxies [11, 18].

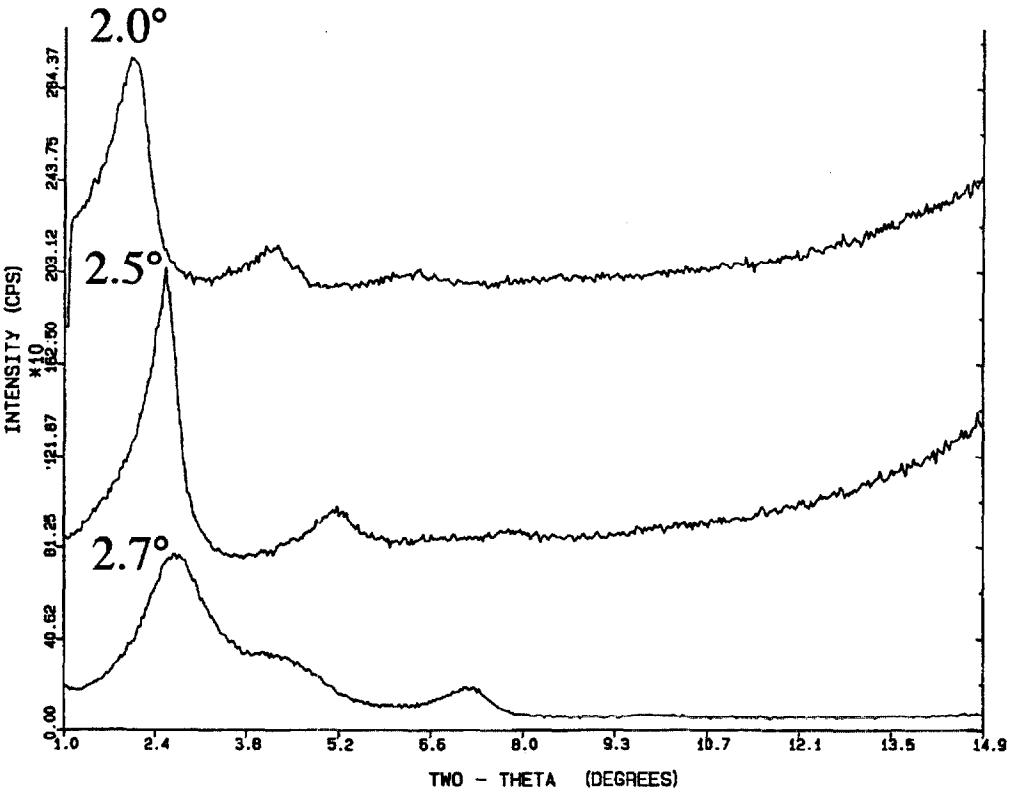

Fig. 14.7 XRD patterns of: pure OMS, dimethyl ditallow ammonium-montmorillonite (*bottom*: $2\theta = 2.7°$, layer spacing 3.3 nm); MDA cured epoxy silicate nanocomposite (*middle*: 6% silicate, $2\theta = 2.5°$, layer spacing 3.5 nm) and BDMA cured epoxy silicate nanocomposite (*top*: 6% silicate, $2\theta = 2.0°$, layer spacing 4.3 nm).

14.6 Epoxy and vinyl ester flammability properties

The results of combustion of the vinyl esters and their respective nanocomposite versions in the cone calorimeter are shown in Table 14.2. Just as with the thermoplastic PLS nanocomposites both the peak and average heat release rates (HRR) were significantly improved for these intercalated vinyl ester nanocomposites with low mass fraction (6%) of silicate. Furthermore, the primary difference (aside from HRR) between the flammability properties of the pure vinyl esters and the nanocomposites is the mass loss rates (MLR). The heat of combustion (H_c), soot (SEA) and carbon monoxide yields are unchanged.

The results of combustion of the MDA/DGEBA and BDMA/DGEBA expoxies and their respective nanocomposite version in the cone calorimeter are shown in Table 14.3. The data show essentially the same behaviour as for the vinyl nanocomposites, about a 40% reduction in peak HRR, average HRR, and average MLR. The heat of combustion (H_c), soot (SEA) and carbon monoxide yields are unchanged. The HRR plots for DGEBA/MDA and the DGEBA/MDA silicate nanocomposite (6%) are shown in Fig. 14.8. This plot is representative of the HRR behaviour for both the epoxies and vinyl esters. Although ignition times in the cone calorimeter are

Table 14.2 Cone calorimeter data for MBA and BAN vinyl esters.

Sample	Residue yield (%) ± 0.5	Peak HRR (Δ%) (kW/m^2)	Mean HRR (Δ%) (kW/m^2)	Mean MLR ($g/s\ m^2$)	Mean H_c (MJ/kg)	Mean SEA (m^2/kg)	Mean CO yield (kg/kg)
Mod-bis-A vinyl ester	0	879	598	26	23	1360	0.06
Mod-bis-A vinyl ester*	8	656 (25%)	365 (39%)	18 (30%)	20	1300	0.06
Bis-A/novolac vinyl ester	2	977	628	29	21	1380	0.06
Bis-A/novolac vinyl ester*	9	596 (39%)	352 (44%)	18 (39%)	20	1400	0.06

Heat flux $35\ kW/m^2$; H_c Heat of combustion; SEA Specific extinction area; MLR Mass loss rate.
* 6% silicate intercalated nanocomposite.

Table 14.3 Cone calorimeter data for DGEBA/MDA and DGEBA/BDMA epoxies.

Sample	Residue yield (%) ± 0.5	Peak HRR (Δ%) (kW/m^2)	Mean HRR (Δ%) (kW/m^2)	Mean MLR ($g/s\ m^2$)	Mean H_c (MJ/kg)	Mean SEA (m^2/kg)	Mean CO yield (kg/kg)
Epoxy resin DGEBA/MDA	11	1296	767	36	26	1340	0.07
Epoxy resin DGEBA/MDA*	19	773 (40%)	540 (29%)	24 (33%)	26	1480	0.06
Epoxy resin DGEBA/BDMA	3	1336	775	34	28	1260	0.06
Epoxy resin DGEBA/BDMA*	10	769 (42%)	509 (35%)	21 (38%)	30	1330	0.06

Heat flux $35\ kW/m^2$; H_c Heat of combustion; SEA Specific extinction area; MLR Mass loss rate.
* 6% silicate intercalated nanocomposite.

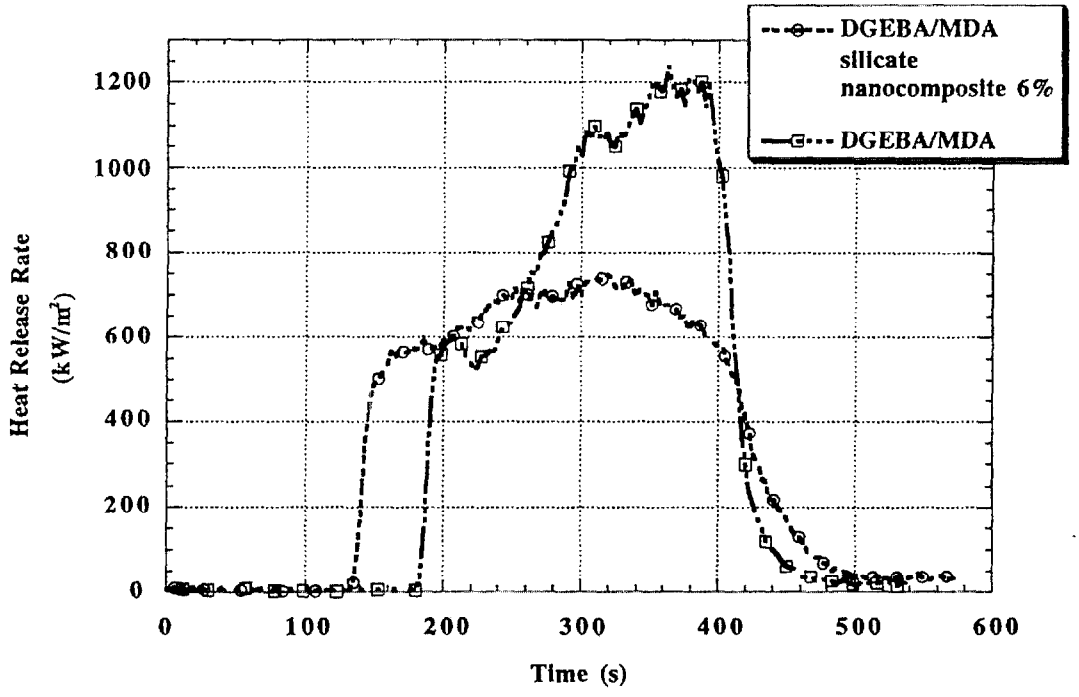

Fig. 14.8 Comparison of the heat release rate (HRR) plots for DGEBA/MDA and DGEBA/MDA silicate nanocomposite (mass fraction 6%) at 35 kW/m^2 heat flux, showing 40% reduction in the peak HRR for the nanocomposite.

accompanied by somewhat large uncertainties (±25%) shorter ignition times are generally observed for the PLS nanocomposites. This may be caused by the low thermal stability of the quaternary alkyl ammonium cation contained in the organic modified montmorillonite used to prepare the PLS nanocomposites.

The data suggest that the source of the improved flammability properties of these materials is due to differences in condensed phase decomposition processes and not to a gas phase effect. As stated above these flammability properties are characteristic of both the thermoplastic and thermoset PLS nanocomposites.

14.7 Char formation and characterization

Comparison of the residue yields for thermoplastics and thermosets reveals little improvement in the carbonaceous char yields, once the presence of the silicate in the residue is accounted for. This was somewhat surprising since other studies of the thermal reactions in layered organic–silicate intercalates, at 400°C, reported formation of carbonaceous–silicate residues and other condensation and crosslinking type reaction products [20]. These data indicate that, although the mechanism of flame retardancy may be very similar for each of the systems studied, it is not via retention of a large fraction of carbonaceous char in the condensed phase. A recent study in our laboratory of the nylon 6 silicate nanocomposite pyrolysis process, in a

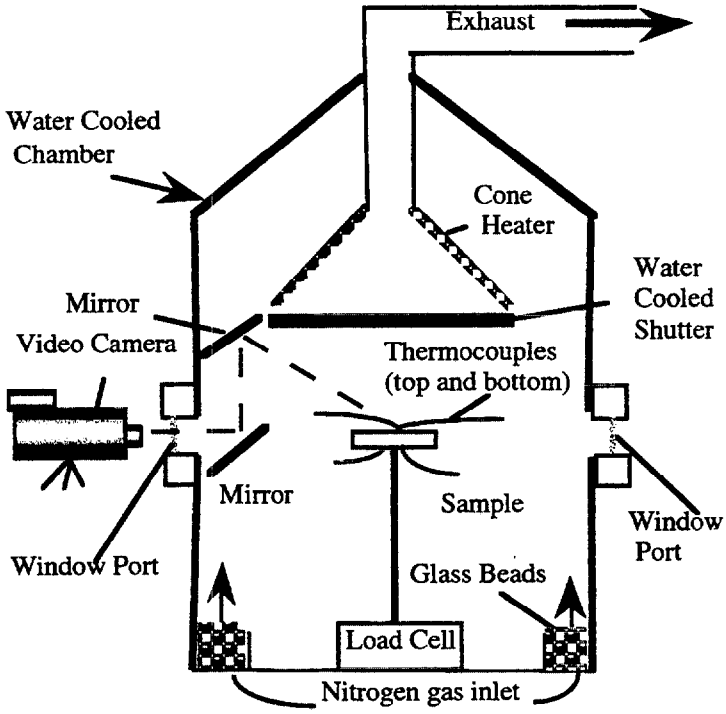

Fig. 14.9 A schematic of the radiative gasification apparatus (1-m diameter, 2-m height). The gasification apparatus allows pyrolysis, in a nitrogen atmosphere, of samples identical to those used in the cone calorimeter.

nitrogen atmosphere, using a radiative gasification apparatus (shown in Fig. 14.9) revealed that the reduction in MLR does not occur until the sample surface is partially covered with char [4]. The MLR data for these N_2 gasification experiments are shown in Fig. 14.10. Visual observation of the pyrolysis shows that at 180 s when the MLR for the nylon 6 silicate nanocomposite slows, compared with the pure nylon 6, the surface of the nanocomposite is over 50% covered by char.

A TEM image of a section of the combustion char from the nylon 6 silicate-nanocomposite (5%) is shown in Fig. 14.11. A multilayered silicate structure is seen after combustion, with the darker, 1 nm thick, silicate sheets forming a large array of fairly even layers. This was the primary morphology seen in the TEM image of the char; however, some voids were also present. The delaminated hybrid structure, appears to collapse during combustion. The nanocomposite structure present in the resulting char appears to enhance the performance of the char through reinforcement of the char layer. This multilayered silicate structure may act as an excellent insulator and mass transport barrier, slowing the escape of the volatile products generated as the nylon 6 decomposes [4]. XRD analysis of chars from combustion of nylon 6, and the two DGEBA nanocomposites (Fig. 14.12) shows that the interlayer spacing of the chars is the same, 1.3 nm, independent of the chemical structure (thermoplastic polyamide, thermoset aromatic diamine cured epoxy or thermoset homopolymerized epoxy) or nanostructure (delaminated or intercalate) of the nanocomposite.

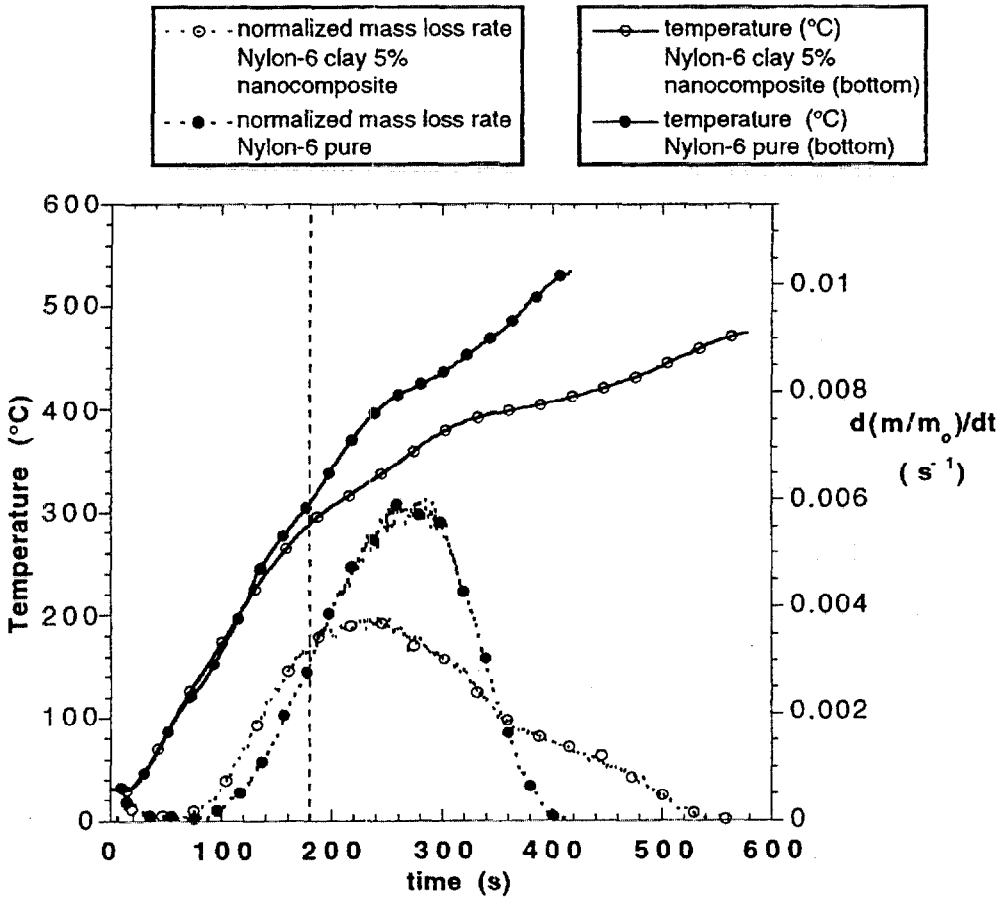

Fig. 14.10 Normalized mass loss rate and temperature *vs.* time plots for the gasification experiments for nylon 6 and nylon 6 silicate (5%) nanocomposites in an N_2 atmosphere. All samples were exposed to a flux of 40 kW/m^2 in an N_2 atmosphere. The mass loss rate curves begin to differ at 180 seconds when the surface of the nanocomposite sample is partially covered by char. The insulating effect of the char can be seen in the bottom-surface thermocouple data for the nanocomposite.

14.8 Conclusions and future trends

The flammability properties of thermoplastic and thermoset polymer layered silicate nanocomposites are reported. The peak and average heat release rate (HRR) are reduced by 40% to 60% in delaminated and intercalated nanocomposites containing a silicate mass fraction of only 2–6%. Not only is this a very promising new method for producing flame retarding polymers, but it does not have the usual drawbacks associated with other additives. That is, the physical properties are not degraded by the additive (silicate); instead they are greatly improved, and the materials are easily recycled. Furthermore, this system does not increase the carbon monoxide or soot produced during the combustion. The nanocomposite structure of the char appears to enhance the performance of the char layer. This layer may act as an insulator and a mass transport barrier slowing the escape of the volatile products generated as the polymer decomposes. The future focus of this project will be on the continued

Fig. 14.11 TEM image of a section of the combustion char from the nylon 6 silicate-nanocomposite (5%) showing the carbon-silicate (1 nm thick, dark bands) multilayered structure. This layer may act as an insulator and a mass transport barrier.

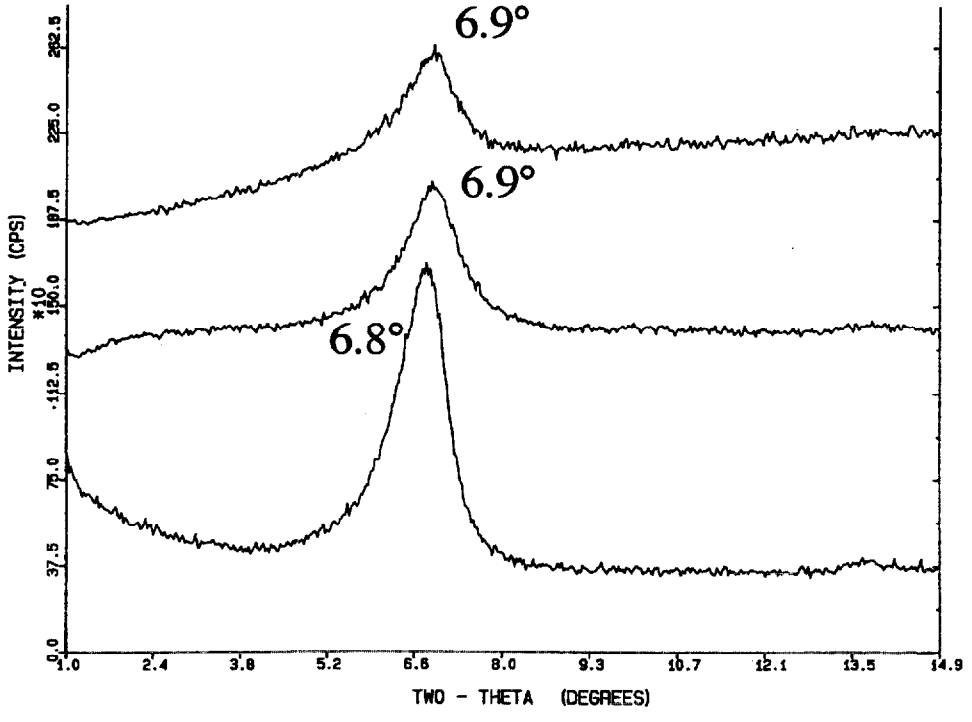

Fig. 14.12 Char XRD patterns of silicate nanocomposites: nylon 6 (*bottom*), DGEBA/BDMA (*middle*), and DGEBA/MDA (*top*). All chars have an interlayer spacing of ~1.3 nm, which is confirmed by TEM images for the nylon 6 nanocomposite char.

development of a fundamental understanding of the fire retardant mechanism of polymer layered silicate nanocomposites. The effect of nanostructure on the flammability properties of a given nanocomposite system will be investigated.

Acknowledgements

The authors would like to thank Dr R. Lyon and the Federal Aviation Administration for partial funding of this work, through Interagency Agreement DTFA0003-92-Z-0018. We would also like to thank Mr Michael Smith for cone calorimeter analysis, Ms Lori Bassel for preparation of vinyl ester and epoxy samples, Dr Doug Hunter and Southern Clay Products for clay samples, and Dr James Cline for use of XRD facilities.

References

1. E.P. Giannelis (1996) *Advanced Materials*, **8**(1), 29.
2. Y. Kojima, A. Usuki, M. Kawasumi, A. Okada, Y. Fukushima, T. Kurauchi and O. Kamigaito (1993) *J. Mater. Res.*, **8**, 1185.
3. J.W. Gilman, T. Kashiwagi and J.D. Lichtenhan (1997) *SAMPE J.*, **33**(4), 40.
4. J.W. Gilman, T. Kashiwagi, S. Lomakin, E.P. Giannelis, E. Manias, J.D. Lichtenhan and P. Jones (1998) In *Fire Retardancy of Polymers: the Use of Intumescence* (G. Camino, M. Le Bras, S. Bourbigot and R. DeLobel, eds), p. 203. The Royal Society of Chemistry, Cambridge.
5. M.S. Wang and T.J. Pinnavaia (1994) *Chem. Mater.*, **6**, 468.
6. A. Usuki, A. Okada and T. Kurauchi (1997) *J. Appl. Polym. Sci.*, **63**, 137.
7. A. Usuki, Y. Kojima, M. Kawasumi, A. Okada, Y. Fukushima, T. Kurauchi and O. Kamigaito (1993) *J. Mater. Res.*, **8**, 1179.
8. J. Lee, T. Takekoshi and E. Gannelis (1997) *Mat. Res. Soc. Symp. Proc.*, Vol. 457, p. 513.
9. J. Lee and E. Giannelis (1997) *Polymer Preprints*, **38**, 688.
10. P.B. Messersmith and E.P. Gianellis (1994) *Chem. Mater.*, **6**, 1719.
11. S. Miyanaga and Y. Tsunoda (1996) Japanese Patent JP 09,255,747.
12. A. Usuki, T. Mizutani, Y. Fukushima, M. Fujimoto, K. Fukamori and O. Kamigaito (1989) U.S. Patent 4,889,885.
13. E.N. Kresge and D.J. Lohse (1997) U.S. Patent 5,665,183.
14. M. Nyden and J.W. Gilman (1997) *Comp. and Theor. Polym. Sci.* **7**, 191.
15. V. Babrauskas and R. Peacock (1992) *Fire Safety Journal*, **18**, 255.
16. V. Babrauskas (1995) *Fire and Materials*, **19**, 243.
17. R.S. Bauer (ed.) (1983) *Epoxy Resin Chemistry II*, ACS Symposium Series 221, American Chemical Society, Washington, DC.
18. C.D. Dudgeon (1987) In *Composites: Engineered Materials Handbook*, Vol. 1, ASM International, Metals Park, OH, p. 90.
19. J.M. Thomas (1982) *Intercalation Chemistry*, Academic Press, London, Ch. 3, p. 55.